High Speed Packaged Electroabsorption Modulators for Optical Communications

Aaron E. Bond, Gleb Shtengel, Prashant Singh, Yuliya Akulova, and C. L. Reynolds, Jr.
Bell Laboratories, Lucent Technologies
RM 1A-231, 9999 Hamilton Blvd., Breinigsville PA 18031, 610-391-2351
abond1@lucent.com, gleb@lucent.com, singhp@lucent.com, yakulova@lucent.com, lr@lucent.com

Abstract

High speed packaged electroabsorption modulators are fabricated from the InGaAsP material system with integrated mode converters. The packaged devices exhibit 43GHz modulation bandwidth, -10dB electrical return loss, and 10dB extinction for 2Vp-p. Device design and package considerations for high speed devices is presented.

Introduction

The fast increase of the bit-rate of the optical fiber communications imposes stringent requirements on components such as transmitters. $LiNbO_3$ Mach-Zehnder (MZ) modulators as well as electroabsorption (EA) modulators are being considered. The requirements include high modulation bandwidth, high extinction ratio, low electrical return loss, and high saturation power. Polarization sensitivity might also be an issue if a device is used at the receiver end. Another important requirement is low drive voltage. The drive voltage must be low owing to limited drive electronics. EA modulators have the advantage over MZ modulators owing to the lower drive voltage critical at 40Gb/s bit rates over.

EA devices with multi-quantum well (MQW) active layers utilize a combination of the quantum-confined Stark effect and the Franz-Keldysh effect, and therefore offer higher extinction ratios than bulk EA modulators. However MQW structures might present problems caused by carrier escape and transport through MQW layers which can decrease the modulation bandwidth and reduce the saturation power.

There have been a number of reports on the realization of EA modulators with a modulation bandwidth in excess of 40GHz in the InGaAlAs material [1] as well as in the InGaAsP system [2,3]. The EA section of the device is kept short to minimize the device capacitance (in most of the reports it is of an order of 100μm). To keep the extinction ratio high, the number of quantum wells is typically increased to 15-20. This also results in the increased thickness of the undoped layer and therefore further reduces the device capacitance. However, devices with such short EA sections cannot be used for practical purposes. Handling such devices is complicated, and stray light degrades the extinction ratio. Placing the EA section between two passive waveguide sections increases the device length. Using the beam-expanders as passive sections also allows for improvement of optical coupling [4].

Modulator design:

Electroabsorption (EA) modulators absorb light passing through the device when a reverse bias is applied across the p-i-n junction. The absorption region in this work is fabricated from the InGaAsP material system with strain compensated quantum wells (QW's) and barriers. The QW EA modulator has enhanced absorption owing to the combined Franz-Keldysh and quantum-confined Stark effects. When no voltage is applied across the p-i-n junction the light is allowed to pass through without being absorbed. Longer absorption regions are advantages for higher extinction ratios, since more light can be absorbed. However, we will demonstrate that longer absorption regions reduce the useful modulation bandwidth.

The modulation bandwidth of the EA modulator is primarily RC limited. Bandwidth decreases with increasing resistance or capacitance. Every effort is made to reduce the size of the EA modulator without compromising the extinction ratio. Unfortunately, as the device size is reduced the overall resistance increases. The tradeoff between extinction ratio and bandwidth has been set by system manufacturers and currently the target is 10dB of extinction for a device with a bandwidth of 40+GHz. These specifications are suitable for the next generation of 40GBit systems.

An experiment was performed to vary the length and width of the EA modulators in this work to determine the optimal device size for 40GBit applications. Two sets of devices were fabricated and tested in which the modulator width and length was varied. One set of devices had a modulator length of 80um and variable widths of 1.4 to 2.8um. The other set of devices had a device length of 120um and variable widths of 1.4 to 2.8um. The extinction characteristics, modulation bandwidth, and electrical return loss were measured.

Modulator fabrication:

The EA modulators were fabricated from the InGaAsP material system and were grown on n+(100) InP substrates in a low-pressure metal-organic chemical vapour deposition system. The multiple quantum well (MQW) modulator structure is composed of strain compensated InGaAsP well material and InGaAsP barrier material. The MQW structure consists of 18 quantum wells and has a PL inflection of 1.51μm.

After MQW epitaxial growth the structure is selectively etched so the final active section of the device will have a device length of 80μm or 120um. Where the MQW is etched away a passive mode converter is grown using selective regrowth. The passive mode convertor is InGaAsP material and is adiabatically tapered over a length of 250um. The entire device is then capped with a thick p-InP cladding layer and a heavily doped p+-InGaAs contact layer. The waveguides are then fabricated in a reactive ion etching (RIE) system based on a CH_4/H_2 etch chemistry. The waveguide width is varied from 1.4-2.8μm in 0.2um steps. The waveguides are RIE etched below the active region for complete electrical isolation. After waveguide formation the

devices are planarized using polyimide and the p and n contacts are deposited. Polyimide is used to planarize the device owing to a low dielectric constant of 3.6. With polyimide the total pad capacitance can be reduced to below 22fF. A cross section of the completed EA modulator is shown in figure 1.

Figure 1: Cross section of the completed EA modulator

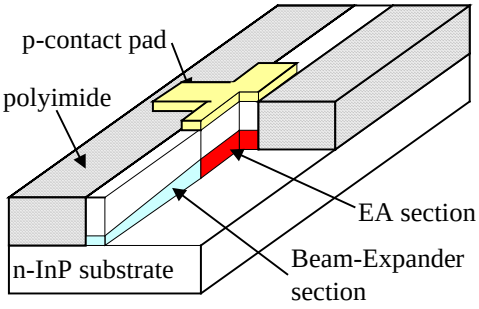

The devices were mounted p-up on submounts with a coplanar electrical waveguide and an integrated matching 50Ω resistor, allowing for high-speed probing with ground-signal-ground probes. We characterized 2 sets of devices with different lengths of the EA sections: 80μm and 120 μm. The total length of the device, including the beam-expander sections, was 600μm for all devices. Within each set of devices, the mesa width varied from 1.4 to 2.8μm (the mesa width is constant along the entire length of the device). We performed DC Extinction measurements as well as high-speed S-parameter characterization. Devices with shorter cavities have lower extinction, but higher small-signal bandwidth and lower electrical return loss. Fiber-to-fiber insertion loss was between 10 and 18dB for most of the devices and was due to facet quality. We did not observe any dependence of the optical insertion loss on the mesa width or active layer length.

Figure 2: DC extinction curves for a 120μm long EA modulator

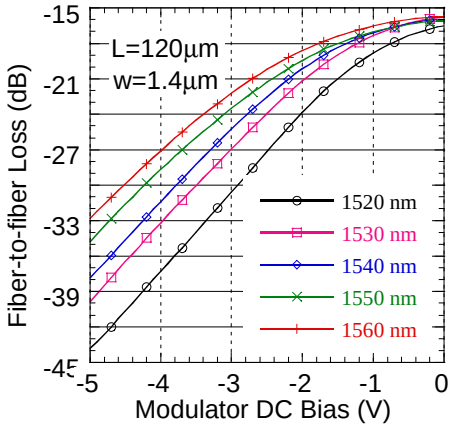

A set of DC extinction curves for a device with 120μm long EA section and a mesa width of 1.4μm is shown in Fig.2. The DC extinction between -1 and -3V is 10dB. This DC extinction was found to be independent of mesa width.

We used an HP8510C Network Analyzer and an HP84330D p-i-n detector to perform the S-parameter measurements. The calibration of the HP84330D detector is accurate only up to ~35GHz. More than half of the devices tested had bandwidth exceeding this value, in this case it is reported as 40GHz.

Shown in Fig.3 is the set of small-signal response (S_{21}) curves for the device in Fig.2 (120μm long EA section and mesa width of 1.6μm), taken at different DC biases. The 3dB bandwidth increases with negative DC bias because the capacitance of reverse-biased p-n junction decreases as the reverse bias increases. At -2V the 3dB bandwidth exceeds 35GHz.

Figure 3: Small signal response (S_{21}) for a 120μm long EA modulator

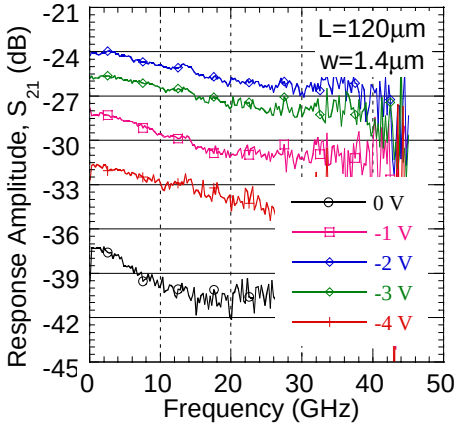

Figure 4: 3dB bandwidth at –2V bias for variable mesa width and length EA modulators

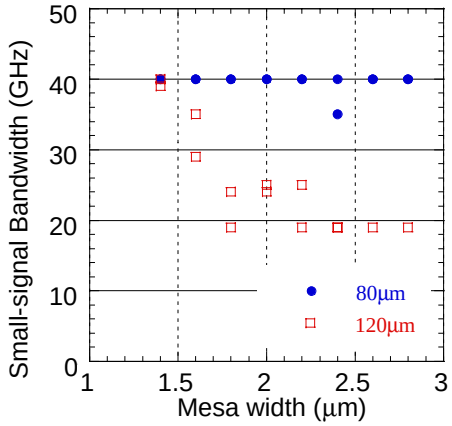

The value of 3dB bandwidth at -2V of DC bias as a function of mesa width for devices with 80μm and 120μm EA sections is plotted in Fig.4. It is known that in order to optimize the EA performance one needs to reduce both series resistance and device capacitance. The series resistance of the EA's is inversely proportional to the mesa area of the device, so it decreases as the mesa width increases. However the device capacitance is proportional to the mesa area, so it increases as the mesa width increases. The 3dB bandwidth of 120μm long devices decreases as the mesa width increases, and the bandwidth of all but one 80μm long device exceeds 35GHz. This trend indicates that for higher modulation bandwidth the low device capacitance is most important, even

if achieved at the expense of increased series resistance. These very high values of bandwidths also allow for conclusion that the carrier transport effects do not limit the device performance.

Figure 5: Electrical return loss (S_{11}) for a 120μm long EA modulator

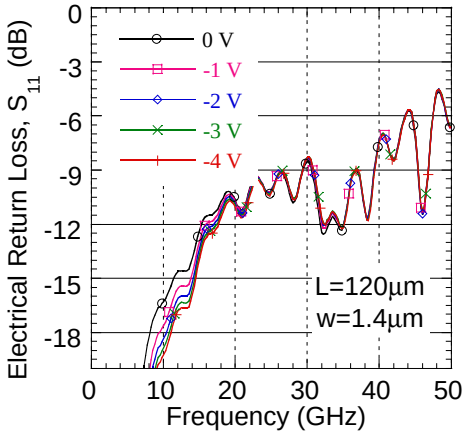

Electrical return loss (S_{11}) as a function of frequency at different DC biases is plotted in Fig.5 (for the EA device in Figs. 2 and 3). The shape of the S_{11} curve is characteristic of the RC equivalent circuit. The amplitude of S_{11} increases with frequency up to 20GHz, and does not change much between 20 and 40GHz. The value of S_{11} at 20GHz and at -1V of DC bias is plotted in Fig.6 as a function of the mesa width for devices with 80μm and 120μm EA sections. The devices with smaller mesas have higher series resistance and lower capacitance. Both effects contribute to reduction of the electrical return loss.

Figure 6: 20GHz electrical return loss for variable mesa width and length EA modulators

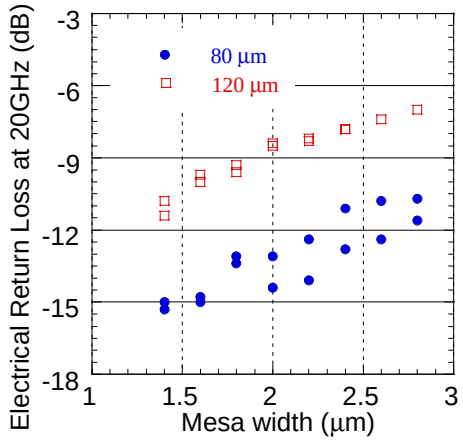

Packaging Considerations

Packaging of high speed electroabsorption modulators involves two primary considerations, the coupling of light into and out of the modulator, and the transfer of the RF drive signal to the modulator. The manner in which these issues are addressed is shown in Figure 7, where a view of the modulator package with the top removed is shown. .

Figure 7: Internal view of a packaged 40GBit EA modulator

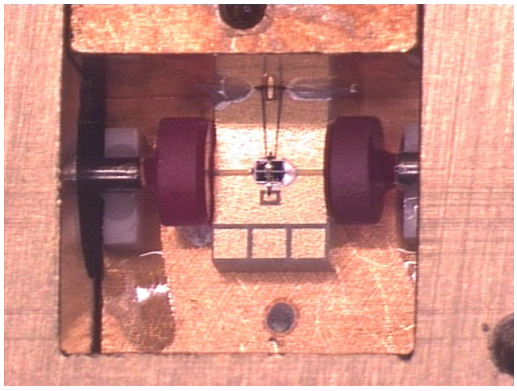

The optical coupling is done through the use of lensed fibers, which are actively aligned to the modulator. The active alignment is done by forward biasing the modulator to generate spontaneous emission, and then maximizing the coupled light. The lensed fibers are brought into the package through metal ferules. A pair of cylindrical ceramic disks are used to support the fiber inside of the package. After the active alignment process, the fibers are epoxied into place.

Figure 8: Layout of the modulator submount

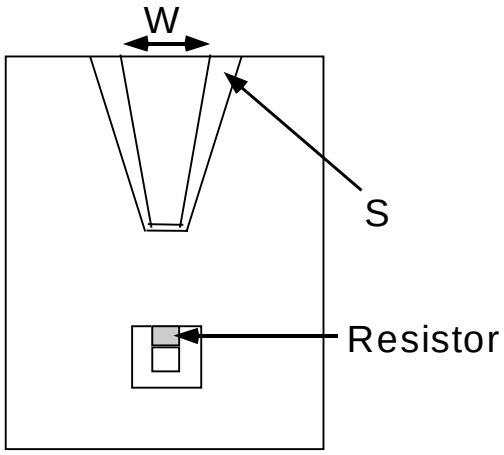

The coupling of the RF signal to the modulator is done through an external V-connector, which is then connected to a coplanar waveguide(CPW) transmission line that is printed on a beryllia (BeO) substrate. The layout of the BeO substrate is shown in Figure 8. The modulator is bonded to the submount using solder. Electrical connections to the modulator are made through ribbon bonds. In addition to having a low RF loss tangent, 0.03 at 10 GHz, BeO also has a very high thermal conductivity, 290W/degrees celcius, which helps with thermal management issues.

In addition to the CPW transmission line, the submount includes a 50Ω thin film termination resistor. The termination resistor is essential for achieving good return loss. The termination resistor is contacted by the use of ribbon bonds. The inductance of the ribbon bond can be used to improve the return loss of the device by resonating out some of the modulators capacitance.

The CPW transmission line is tapered. The wide portion of the taper allows for the connection of the V-connector, and the narrow portion of the taper improves high frequency performance. The CPW transmission line was designed to have a 50 Ω characteristic impedance. The dimensions of the transmission line were calculated using LINPAR, a 2-dimensional method of moments based electromagnetic solver. The dimensions at the input and output of the transmission line were computed, and a polygon was used to connect the points. For the use of the reader, Table 1 is provided to list the dimensions that are necessary to achieve a 50 Ω CPW transmission line in BeO, which has a relative dielectric constant,ε_r, of 6.7.

Table 1: CPW transmission line dimensions on BeO. W is the width of the center conductor, and S is the spacing between the edge of the center conductor and the edge of the ground plane.

W (mils)	S (mils)	Z_{real} (Ω)	Z_{imag} (Ω)	Attenuation (dB/cm)	Phase Velocity (cm/s)
12	3	50.28	0.41	0.608	1.559×10^{10}
9	2.5	51.31	0.37	0.645	1.555×10^{10}
5	1.4	50.44	0.17	0.778	1.557×10^{10}
3	1	52.15	-0.04	0.910	1.565×10^{10}

The quality of the transmission line can be determined by extracting the characteristic impedance and attenuation from a measurement of the 2-port scattering parameters. The two port S-parameters can be transformed into equivalent impedances of open and short circuit stubs through the application of Mason's Rule.

$$\Gamma_{oc} = S_{11} + \frac{S_{12}S_{21}}{1 - S_{22}} \qquad (1)$$

$$\Gamma_{sc} = S_{11} - \frac{S_{12}S_{21}}{1 + S_{22}} \qquad (2)$$

$$Z_{oc} = 50\frac{1 + \Gamma_{oc}}{1 - \Gamma_{oc}} \qquad (3)$$

$$Z_{sc} = 50\frac{1 + \Gamma_{sc}}{1 - \Gamma_{sc}} \qquad (4)$$

The characteristic impedance, propagation constant, and attenuation of the CPW can then be calculated from the impedances of the open and short circuit stubs.

$$Z_{line} = \sqrt{Z_{oc} \cdot Z_{sc}} \qquad (5),$$

$$\gamma = \alpha + j\beta = \frac{1}{L}\operatorname{atan}\left(\frac{Z_{sc}}{Z_{line}}\right) \qquad (6),$$

$$Attenuation(dB) = 8.686 * \alpha \qquad (7),$$

where L is the length of transmission line. The results of these measurements are shown in Figure 9. The CPW transmission line has an impedance close to 50Ω up to 40 GHz, and a low attenuation, less than 3 dB/cm at 40 GHz.

Figure 9. Measured characteristic impedance and attenuation of the CPW transmission line.

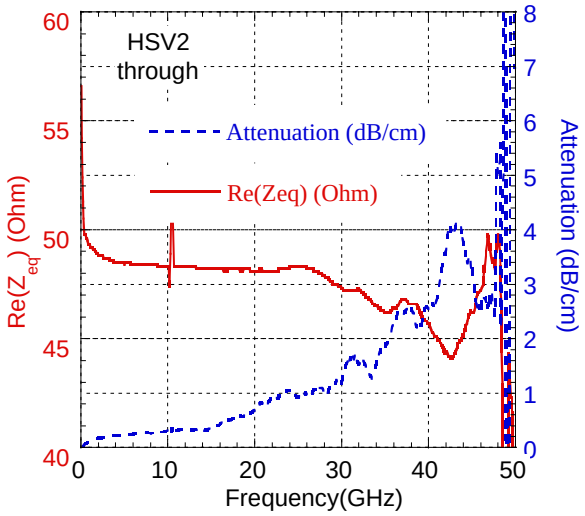

Measurements of the return loss, bandwidth, and optical eye diagram of the packaged modulator shows that the package is free of resonances. The package described here provides an electrically and optically neutral environment in which the place the modulator. As a result, the performance of the packaged modulator is dominated by the properties of the modulator chip itself, rather than by the package.

Packaged Results

The small signal modulation bandwidth was measured for the packaged EA devices using an HP8510C 50GHz network analyzer and a calibrated HP photodetector. All packaged device measurements were taken with lensed single mode fibers for optical coupling, and a Wiltron-V connector for launching the microwave signal through the package wall. The complete package is shown in figure 10.

Figure 11 shows a plot of the small signal modulation as a function of frequency for an 80μm long modulator operated with an input optical power of 6dBm @1530nm and an electrical modulation of –8dBm. The small signal response curves show a 3dB bandwidth of 43GHz for bias voltages from –2.0V to –4V.

Figure 10: Picture of packaged electroabsorption modulator with Wiltron-V connector

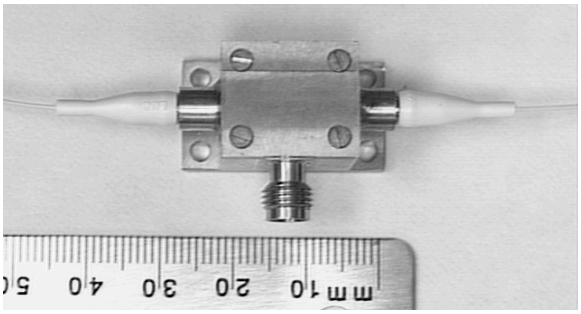

The electrical return loss is an important parameter when a device is used in a real system with a driver circuit. The electrical return loss should be kept to a minimum for optimum RF performance. The electrical return loss for an 80μm long modulator is shown in figure 12. The electrical return loss is below –7.5dB for frequencies up to 40GHz.

Figure 11: Small signal modulation response of a packaged 80μm EA modulator with integrated mode converters

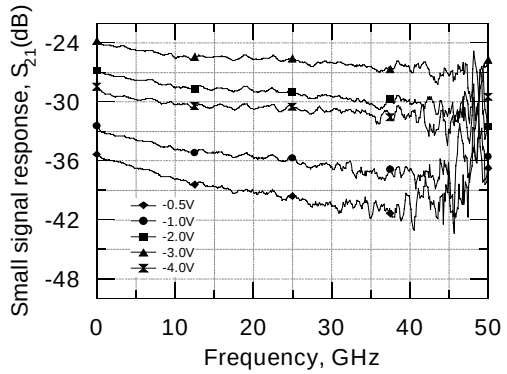

Figure 12: Electrical return loss from a packaged 80μm EA modulator with integrated mode converters

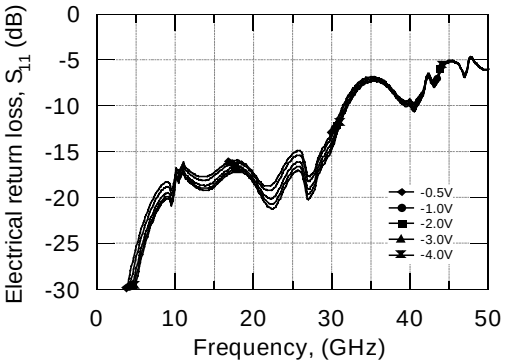

The fiber to fiber insertion loss for devices which do not include beam expanders is greater than 30dB. This is unacceptable for real systems. The insertion loss of our packaged device with integrated mode converters was measured to be 15dB @1530nm. The extinction curves as a function of reverse bias is shown in figure 13. An overall extinction of 20dB for 5V was obtained even with an 80μm long modulator. The sharpness of the extinction curve and the total insertion loss is a subject of continued research and should be improved in future work.

The eye diagram of a high speed EA modulator measured at 40Gb/s is shown in figure 14. The RF extinction for 2.0Vp-p at 40Gb/s was 6.0dB, which is similar to the DC extintion indicating these devices are not bandwidth limited.

Figure 13: Optical insertion loss as a function of reverse bias for an 80μm long EA modulator

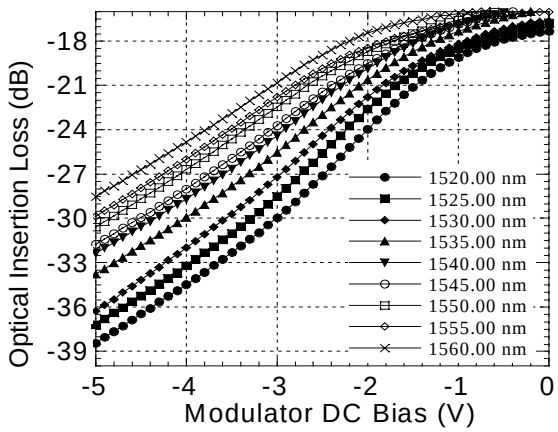

Figure 14: 40Gb/s electrical (top) and optical (bottom) eye diagram for 2Vp-p drive voltage.

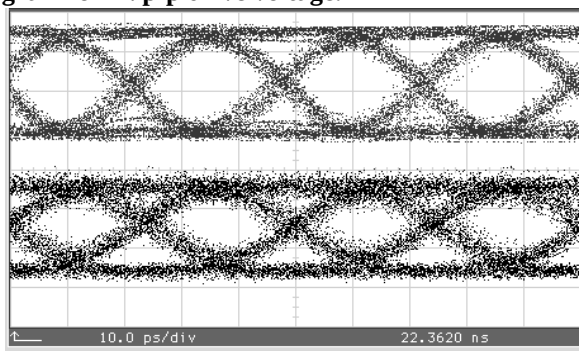

Conclusions

The design of electroabsorption modulators was reviewed and an experiment to vary the length and width of EA modulators was performed. The capacitance was clearly shown to be the limiting factor in high speed response even at the expense of higher resistance. Packaged EA modulators operated at 40GBit/s with an RF extinction of 6dB for 2V.

Acknowledgments

The authors would like to acknowledge Ron Leibenguth, Ken Glogosky, Kevin Dreyer, and Brian Falk for their contributions to this work.

References

1. Wakita, K., et al, *IEICE Trans. Electron.*, Vol. E81-C, No. 2, pp. 175-79, 1998.
2. Satzke, K., et al, *Electron. Lett.*, Vol. 31, No. 23, pp. 2030-32, 1995.
3. Takeuchi, H., et al, *IEEE Photon. Technol. Lett.*, Vol. 9, No. 5, pp. 572-574, 1997.
4. Ido, T., et al, *IEEE Photon. Technol. Lett*., vol.7, No. 2, pp.170-172, 1995.